Leak Detection And Spatial Localization of Leaks Inside Fusion Devices

Ghassan Antar[1], Priyanka Jena[2*], Thierry Alarcon[3], Philippe Moreau[3], Eric Caprin[3], Martin Kocan[2], Liam Worth[2], Graeme Vine[2], Robert Pearce[2], Didier Mazon[3], Vincent Martin[2], and Roger Reichle[2]

[1] American University of Beirut, Physics Department, Riad El-Solh, Beirut 1107 2020, Lebanon
[2] ITER Organisation, Route de Vinon-sur-Verdon, CS 90 046, 13067 St. Paul Lez Durance Cedex, France
[3] *CEA, IRFM F-13108, Saint Paul Lez Durance, France*
*Presenting author: priyanka.jena@iter.org

1. Introduction

A fusion device, such as tokamaks, requires a high vacuum (1×10^{-5} Pa) to create and sustain a high-performance plasma. [1]. A leak as small as 10^{-6} Pa·m^3·s^{-1} of either air or water compromise the high-vacuum condition and could impede the operation of a fusion device [2]. Detecting the existence of a leak can be done using pressure gauges but identifying which component is leaking could take several weeks in present day tokamaks like ITER. Hence, there is a pressing need to develop methodologies for quick spatial localization of micro-metric leaks. In order to address this issue, an approach has been devised for the detection and localization leaks using glow discharge cleaning (it is a method of conditioning vacuum vessel walls using a low temperature unmagnetized plasma discharge [3]) together with visible spectroscopy and visible imaging. To demonstrate the feasibility of our approach, experiments are being carried out. This contribution presents the experimental setup as well as the first encouraging results of the experiments.

2. Experimental Setup

The experimental test bed consists of a Helium glow discharge device installed in a vacuum vessel with an arrangement for calibrated water and air leak. A residual gas analyzer (RGA), and a visible spectrometer are used to detect the leak. Fig. 1 shows the schematic representation of the experimental test bed where the glow discharge is done using Helium.

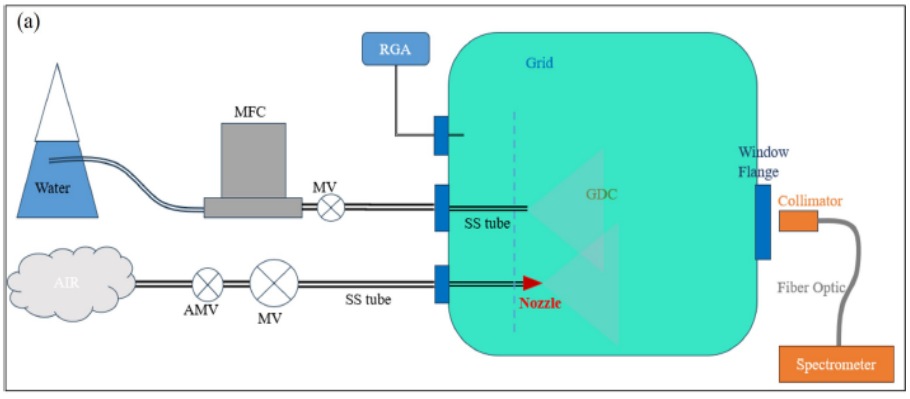

Figure 1. Schematic of experimental test bed with the possibility to introduce an air or a water leak using respectively an Manual Valve (AMV) and an Mass-flow controller (MFC) positioned before a manual valve (MV). Water leak is puffed through a stainless steel tube, for the air leak we install a nozzle. The collimator of the spectrometer allows the view of the two leaks

3. Air leak signature using the visible spectrometer

In Fig. 2 we plot the spectrum of light in the visible range when the calibrated air leak valve is closed and when it is set to the smallest graduation. The integration time of the spectrometer was set to 2 seconds. It is clear that even for the smallest leak, an increase in the amplitude of the spectrum is detected.

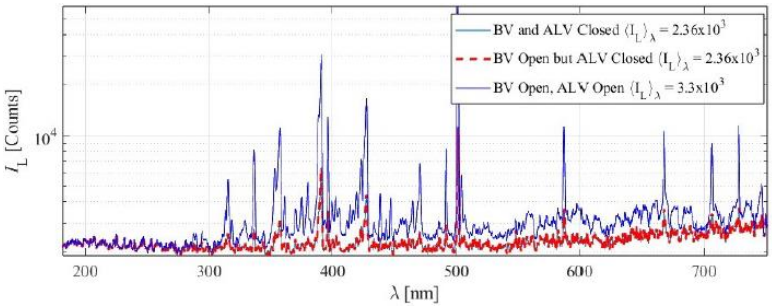

Figure 2. Intensity versus wavelength recorded by visible spectrometer when the air leak valve is closed (dashed red) and when it is open (solid blue)

The RGA allowed us to obtain the partial pressure for Helium as well as components of air and water like Hydrogen, Oxygen and Nitrogen. The dependence of the visible spectra for the four species at different air leak rate with respect to the partial pressure of nitrogen (P_{N2}) is shown in Fig. 3. It is observed that the spectral lines show a significant increase even at low leak rate. At the smallest leak rate, the increase is important and assessed using ΔI_α where α indicates the different lines used, namely Nitrogen, Oxygen, Helium, and Hydrogen lines. The dependence on P_{N2} is assumed to follow a power law with a scaling exponent being ξ_α. It is observed that the scaling component of Oxygen (ξ_O)is the highest, followed by Hydrogen and Nitrogen.

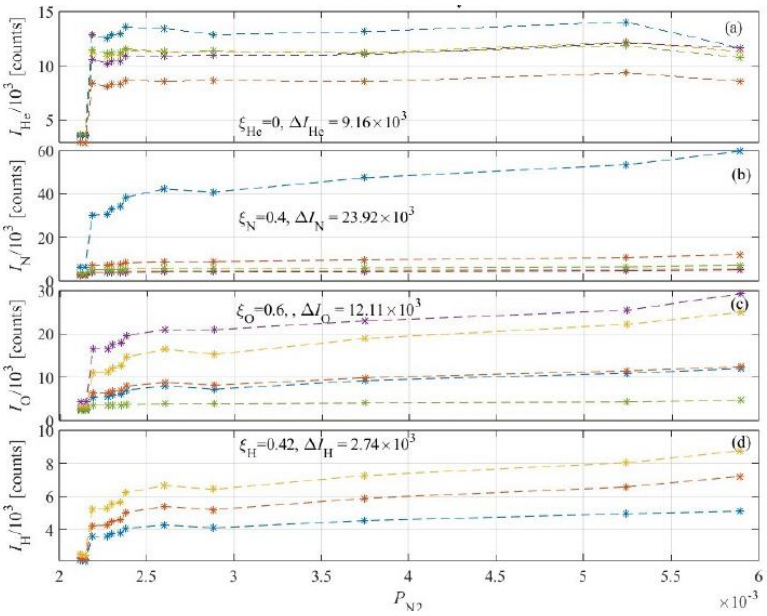

Figure 3. Spectral response of different elements with respect to nitrogen partial pressure. The jump of the light intensity ΔI_α is shown for each element $\alpha = \mathrm{N}, \mathrm{H}, \mathrm{O}$, and He determined as the difference between no

leak and the smallest achievable leak. The rate of increase of the light intensity of the different species is assumed to follow the power law P_{N2}^{ξ} with ξ for the different elements is shown.

4. Water leak test

Fig. 4 shows the spectrum when the calibrated water leak valve is closed and when it is set to the smallest possible leak of about $\Phi_{H2O} = 15$ mg/hr (corresponds to 3%). As with air, a small water leak shows a strong growth in the amplitude over the entire spectrum.

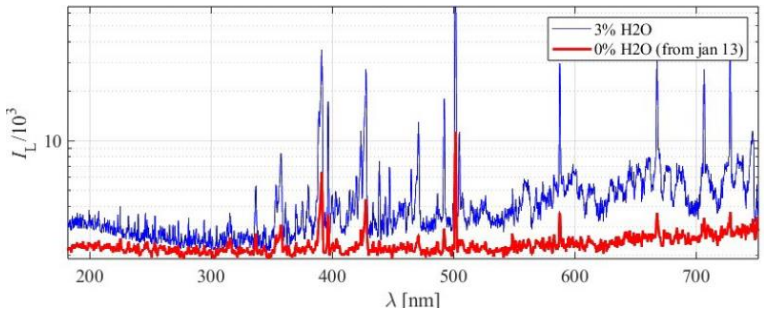

Figure 4. Intensity versus wavelength recorded by visible spectrometer during water leak

Fig. 5 shows the average peak intensities obtained from the light spectrum of the various elements as a function of the leak rate. It is observed that the Helium lines shows the highest increase in intensity (in comparison to other elements) at a leak rate of 40 mg/hr. The next best indicator of water leak is Hydrogen, followed by Nitrogen and Oxygen.

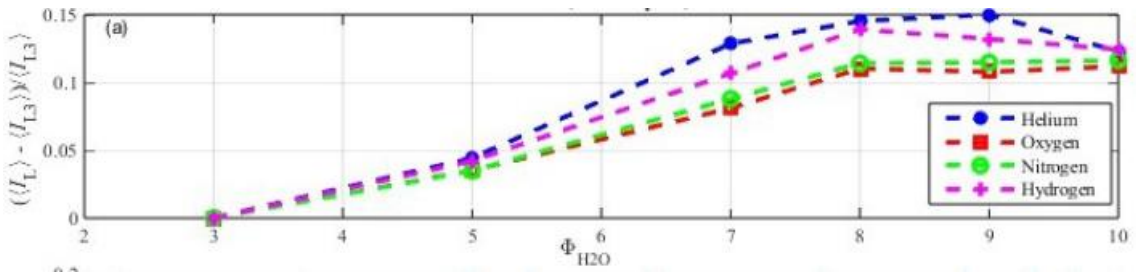

Figure 5. Average peak intensity of the four elements normalized to the values obtained with the smallest leak as a function of the Φ_{H20}.

5. Effect of spatial variation on water leak detection

The spectrometer is equipped with a fiber optic linked to a collimator. The dependence of the results on the angle of the collimator θ allows us to assess how critical a direct view is when trying to assess the spatial position of the water/air leak. Fig. 6 shows the normalized average intensity of the different elements as a function of collimator angle. For a distance of 1 m between the collimator and the nozzle, an angular deviation of 15° leads to a distance of about 25 cm. The results indicate that the amount of light recorded for the various elements depends on θ but the decrease of the light intensity is mild allowing a possible detection of the water/air leaks even though the camera is not directly looking at it.

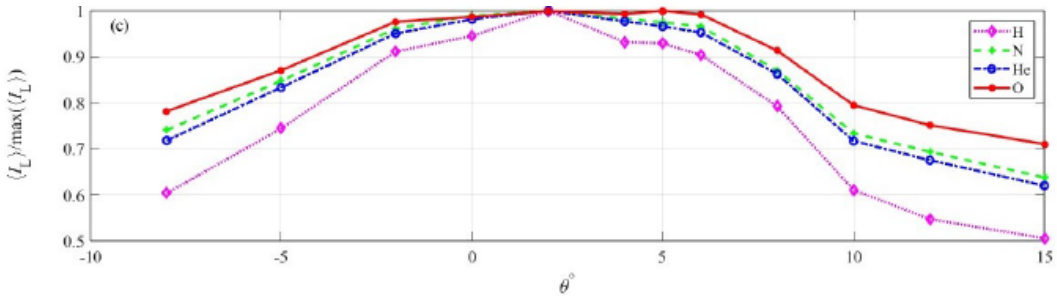

Figure 6. Average peak intensity of the four elements plotted as a function of the collimator angle θ.

6. Summary

The following observations are made from the experiments:

1. The minimum detection limit is well below the minimum leak rate considered here for both air and water leak. This indicates that smaller leaks can also be detected.
2. Spectral lines related to Hydrogen, oxygen, Nitrogen and Helium are excited leading to intensities greater than the background. Their intensities depend on the leak rate, thus increasing when the latter is increased.
3. The spectrum is found sensitive to the orientation or position of the measurement device relative to the source. This indicated that the accuracy of localization of the leak has a dependence on detector position with respect to the leak location.

These results allow us to be optimistic about the possibility to detect the spatial position of leaks in a tokamak using a combination of glow discharge and visible imaging, both available on different devices and on ITER in particular.

7. References

1. L. Wang, Y.H. Zhang, Q. Hu, X.M. Wang, X. Zhang, J. Hu, Y. Yang, X. Gu, Design and construction of vacuum control system on EAST, Fusion Engineering and Design, Volume 83, Issues 2-3, 2008, Pages 295-299.
2. Au. Durocher, V. Bruno, M. Chantant, L. Gargiulo, T. Gherman, J.-C. Hatchressian, M. Houry, R. Le, D. Mouyon, Remote leak localization approach for fusion machines, Fusion Engineering and Design, Volume 88, Issues 6–8, 2013, Pages 1390-1394.
3. D. Kogut, D. Douai, G. Hagelaar, R.A. Pitts, Modelling the ITER glow discharge plasma, Journal of Nuclear Materials, Volume 463, 2015, Pages 1113-1116.